

Accepted Manuscript

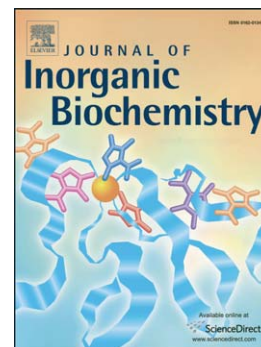
G-quadruplex vs. duplex-DNA binding of nickel(II) and zinc(II) Schiff base complexes

Riccardo Bonsignore, Alessio Terenzi, Angelo Spinello, Annamaria Martorana, Antonino Lauria, Anna Maria Almerico, Bernhard K. Keppler, Giampaolo Barone

PII: S0162-0134(16)30133-7
DOI: doi: [10.1016/j.jinorgbio.2016.05.010](https://doi.org/10.1016/j.jinorgbio.2016.05.010)
Reference: JIB 9999

To appear in: *Journal of Inorganic Biochemistry*

Received date: 5 February 2016
Revised date: 21 April 2016
Accepted date: 13 May 2016



Please cite this article as: Riccardo Bonsignore, Alessio Terenzi, Angelo Spinello, Annamaria Martorana, Antonino Lauria, Anna Maria Almerico, Bernhard K. Keppler, Giampaolo Barone, G-quadruplex vs. duplex-DNA binding of nickel(II) and zinc(II) Schiff base complexes, *Journal of Inorganic Biochemistry* (2016), doi: [10.1016/j.jinorgbio.2016.05.010](https://doi.org/10.1016/j.jinorgbio.2016.05.010)

This is a PDF file of an unedited manuscript that has been accepted for publication. As a service to our customers we are providing this early version of the manuscript. The manuscript will undergo copyediting, typesetting, and review of the resulting proof before it is published in its final form. Please note that during the production process errors may be discovered which could affect the content, and all legal disclaimers that apply to the journal pertain.

G-quadruplex vs. duplex-DNA binding of nickel(II) and zinc(II) Schiff base complexes

Riccardo Bonsignore,^{a,b} Alessio Terenzi,^{c,d} Angelo Spinello,^{a,b} Annamaria Martorana,^a Antonino Lauria,^a Anna Maria Almerico,^a Bernhard K. Keppler,^{c,d} Giampaolo Barone^{*a,b}

^a Dipartimento di Scienze e Tecnologie Biologiche, Chimiche e Farmaceutiche, Viale delle Scienze, Edificio 17, 90128 Palermo, Italy.

^b Istituto EuroMediterraneo di Scienza e Tecnologia, Piazzetta Briuccia, 20-21, 90139 Palermo, Italy.

^c Institute of Inorganic Chemistry, University of Vienna, Währingerstr. 42, A-1090 Vienna, Austria.

^d Research Platform “Translational Cancer Therapy Research”, University of Vienna and Medical University of Vienna, Vienna, Austria.

* Corresponding author: E-mail: giampaolo.barone@unipa.it; Fax: +39 091 596825.

Abstract:

Novel nickel(II) (**1**) and zinc(II) (**2**) complexes of a Salen-like ligand, carrying a pyrimidine ring on the N,N' bridge, were synthesized and characterized. Their interaction with duplex and G-quadruplex DNA was investigated in aqueous solution through UV-visible absorption, circular dichroism and viscometry measurements. The results obtained point out that, while the zinc(II) complex does not interact with both duplex and G-quadruplex DNA, the nickel(II) complex **1** binds preferentially to G-quadruplex respect to duplex-DNA, with values of the DNA-binding constants, K_b , $2.6 \times 10^5 \text{ M}^{-1}$ and $3.5 \times 10^4 \text{ M}^{-1}$, respectively. Molecular dynamics simulations provided an atomic level model of the top-stacking binding occurring between **1** and *hTelo* G-quadruplex.

Keywords: Binding Constant; Circular Dichroism; Computational Chemistry; DNA G-quadruplex, Nickel; Zinc

1. INTRODUCTION

First row metal complexes of Schiff base ligands possess interesting and tunable DNA-binding properties [1–3], ranging from DNA-intercalation to groove binding, depending on the size and shape of the ligand and on the nature of the coordinated metal ion.

In the last 10 years, our research group has investigated on several transition metal complexes of ligands generated by the condensation of a chosen diamine and a modified salicylaldehyde, within what is known as Metal-Salen chemistry [4]. In particular, by changing the diamine and the central ion we obtained compounds with different affinity for DNA and with diverse binding modes. For example, an iron(III) Salen complex shows groove binding properties [5], while nickel(II), copper(II) and zinc(II) Salphen derivatives are DNA intercalators [6–8]. The zinc(II)-Salphen-like complex showed interesting photochemical properties, being the fluorescent emission of the photooxydized product drastically quenched by the DNA-intercalation process [9–11].

Computational chemistry has played an important role in our research, for supporting the interpretation of solution absorption and emission spectra, and for providing atomistic models for the DNA-binding mechanism [10–13].

Recently, also inspired by the work of Vilar, Aldrich-Wright, Neidle, and coworkers [14–17] on similar metal complexes, our interest has moved toward the search for novel Schiff base complexes as selective G-quadruplex binders [13].

G-quadruplexes (G4) are non canonical secondary DNA structures, arising from guanine-rich sequences, in which four guanines are linked by Hoogsteen hydrogen bonds thus creating tetrads that are stabilized both by π - π stacking interactions between them, and by the presence of a cation (usually K^+) coordinated to O6 of the guanines. Recently, these structures have been found to occur in human cells, especially in guanine-rich sequences found in telomeric and in

proto-oncogene promoting regions of the polynucleotide [18,19] such as c-Kit, KRAS, PDGF-A and c-Myc [20–22]. It has been proposed that G4 folding has a regulatory mechanism for the transcription of these genes, whose expression is associated with the occurrence of cancer and that their stabilization as G4-DNA by designed molecules might lead to block their transcription and have remarkable activity in anticancer therapy [20]. Moreover, human telomeric DNA is known to shorten during cells replications until a limit length when cells enter senescence and induce their own apoptosis. Nevertheless, some cells as stem ones overcome the telomeric-shortening induced apoptosis by means of a reverse transcriptase enzyme, namely the telomerase, capable to catalyse the elongation of the telomeres. Unluckily, its overexpression in cancer cells grants them infinite proliferative capabilities [23]. In such a context, the stabilization of the telomeres as guanine quadruplex by means of small binders could inhibit telomerase activity and therefore become a powerful strategy for anticancer treatments [13,15]. Notably, for the structural differences between G-quadruplex and duplex-DNA, a molecule that exhibit a selective interaction with G4 rather than duplex-DNA, might have less toxic effects and might also be more suitable for treatments.

As a continuation of our research in this field, here we report on the synthesis of two novel nickel(II) (**1**) and zinc(II) (**2**) complexes of a Salen-like derivative, presenting a pyrimidine moiety on the N,N' bridge (see Scheme 1) and on the study of their binding properties with both duplex and G-quadruplex DNA.

2. MATERIALS AND METHODS

General. Solvents and reagents (reagent grade) were all commercially available and used without further purification. The 5-(triethylammoniummethyl)salicylaldehyde chloride ligand was prepared from 5-chloromethyl salicylaldehyde and triethylamine in tetrahydrofuran, as recently reported [12]. ^1H and ^{13}C NMR spectra were recorded in DMSO- d_6 solution, with TMS as an internal reference, on a Bruker Avance 500 and 125 MHz NMR spectrometer. Mass

spectra were recorded on Bruker Maxis Classic ESI Qq TOF. IR spectra were recorded on a Jasco FT-IR 420 spectrometer. NMR, IR, MS spectra are reported in the Supplementary material. UV-vis spectra were collected on a Varian UV-vis Cary 1E double beam spectrophotometer equipped with a Peltier temperature controller. Circular dichroism spectra were recorded on a Jasco J-715 spectropolarimeter. 1 cm path-length quartz cuvettes were used. Viscosity measurements were performed on an Ubbelodhe viscometer maintained at 25.0 ± 0.1 °C. The flow time was measured with a digital stopwatch.

Synthesis

1: 5-(triethylammoniummethyl)salicylaldehyde chloride (136.5 mg, 0.50 mmol) was dissolved in H₂O and added to a water solution of 4,5-diaminopyrimidine (27.6 mg, 0.25 mmol). To the resulting mixture, 26.5 mg (0.25 mmol) of Na₂CO₃ and a water solution of Ni(ClO₄)₂·6H₂O (94.3 mg, 0.25 mmol) were added. The resulting mixture was stirred overnight at room temperature. The brilliant red precipitate was washed with cold ethanol, water and diethyl ether, to afford the compound as brown red solid (yield 110.0 mg, 55%).

¹H NMR δ (ppm): 1.24–1.32 (m, 18H, CH₃); 3.16–3.22 (m, 12H, CH₂); 4.37 (d, 4H, CH₂, J = 25 Hz); 6.81 (s, 2H, Ar); 7.88 (s, 1H, Ar); 8.14 (s, 2H, Ar); 8.76–9.33 (m, 3H, Ar); 10.19 (s, 1H, CH); 10.30 (s, 1H, CH).

m/z = 301.1429

Elemental analysis for C₃₂H₄₈Cl₂N₆O₁₂Ni (**1**, 2ClO₄⁻·2H₂O). Found.; C, 45.84%, H, 5.77%, N, 10.02%; calc.: C, 45.43%, H, 5.57%, N, 10.54%.

IR: ν (C=N) 1624 cm⁻¹; ν (O–Ni) 518 cm⁻¹; ν (N–Ni) 459 cm⁻¹.

UV [nm (ε, M⁻¹ cm⁻¹): 238 (4.96 × 10⁴), 259 (3.36 × 10⁴), 368 (1.26 × 10⁴).

2: 5-(triethylammoniummethyl)salicylaldehyde chloride (136.7 mg, 0.51 mmol) was dissolved in H₂O and added to a water solution of 4,5-diaminopyrimidine (26.9 mg, 0.24 mmol). To the

resulting mixture it was added triethylamine (69.7 μL , 0.50 mmol) and a water solution of $\text{Zn}(\text{ClO}_4)_2 \cdot 6\text{H}_2\text{O}$ (94.5 mg, 0.25 mmol). The resulting mixture was stirred for 4 h at room temperature. The brilliant orange precipitate was washed with cold ethanol, water and diethyl ether, to afford the compound as an orange solid (yield 124.2 mg, 61%).

^1H NMR δ (ppm): 1.26–1.39 (m, 18H, CH_3); 3.09–3.23 (m, 12H, CH_2); 4.35 (d, 4H, $J = 15$ Hz CH_2); 6.80 (d, 1H, $J = 5$ Hz, Ar); 6.82 (d, 1H, $J = 5$ Hz, Ar); 7.33–7.37 (dd, 1H, $J_1 = 5$ Hz, $J_2 = 10$ Hz, Ar); 7.39–7.42 (dd, 1H, $J_1 = 5$ Hz, $J_2 = 10$ Hz, Ar) 7.50–7.51 (d, 1H, $J = 2.5$ Hz, Ar); 7.69–7.70 (d, 1H, $J = 5$ Hz, Ar); 8.99 (s, 1H, Ar); 9.24 (s, 1H, Ar); 9.35 (s, 1H, CH); 9.54 (s, 1H, CH).

^{13}C NMR δ (ppm): 7.5 (CH_3), 45.7 (CH_2), 51.3 (CH_2), 51.5 (CH_2), 59.4 (CH_2), 111.4 (Ar), 112.0 (Ar), 118.8 (Ar), 119.4 (Ar), 124.2 (Ar), 124.7 (Ar), 131.9 (Ar), 138.0 (Ar), 139.2 (Ar), 141.0 (Ar), 142.7 (Ar), 146.6 (Ar), 155.3 (Ar), 155.4 (Ar), 164.7 (CH), 165.3 (CH), 173.5 (Ar), 175.4 (Ar).

$m/z = 304.1402$

Elemental analysis for $\text{C}_{32}\text{H}_{46}\text{Cl}_2\text{N}_6\text{O}_{11}\text{Zn}$ (**2**, $2\text{ClO}_4^- \cdot 1\text{H}_2\text{O}$). Found: C, 46.47%, H, 5.61%, N, 10.16%; calc.: C, 46.92%, H, 5.89%, N, 10.30%.

IR: ν (C=N) 1618 cm^{-1} ; ν (O–Zn) 530 cm^{-1} ; ν (N–Zn) 478 cm^{-1} .

UV [nm (ϵ , $\text{M}^{-1}\text{ cm}^{-1}$)]: 238 (5.42×10^4), 275 (1.95×10^4), 385 (1.10×10^3).

UV-vis studies

Lyophilized calf thymus DNA (Fluka, BioChemika) was resuspended in 1.0 mM tris-hydroxymethyl-aminomethane (Tris-HCl) pH=7.5 and dialyzed as described in the literature [24]. DNA concentration, expressed in monomers units ($[\text{DNA}_{\text{phosphate}}]$), was determined by UV spectrophotometry using $6600\text{ M}^{-1}\text{ cm}^{-1}$ as molar absorption coefficient at 260 nm [25]. All experiments were carried in 100 mM KCl, 50 mM Tris-HCl aqueous buffer at pH =7.4.

The 22-mer sequence oligonucleotide *hTelo*: 5'-AGGGTTAGGGTTAGGGTTAGGG-3' was purchased from BioGenerica BioTechnology (Italy). The oligonucleotides were dissolved in MilliQ water to yield a 100 μM stock solution. These were then diluted using 50 mM Tris-HCl/100 mM KCl buffer (pH 7.4) to the desired concentration. The oligonucleotide was folded by heating the solutions up to 90 $^{\circ}\text{C}$ for 5 min and then by slowly cooling at room temperature. The complexes were dissolved in 50 mM Tris-HCl/100 mM KCl buffer (pH = 7.4) to the appropriate concentrations. Concentration of the oligonucleotide solutions was further checked measuring their absorbance and using the appropriate extinction coefficients, *hTelo*, $\epsilon_{260} = 259 \text{ mM}^{-1} \text{ cm}^{-1}$, as reported in the products labels by Bio-Generica BioTechnology.

UV-vis absorption spectra were recorded at 25 $^{\circ}\text{C}$. The titrations were carried out adding increasing amounts of DNA (duplex-DNA or oligonucleotides) stock solution to a metal-complex solution with constant concentration. To ensure that during the titration the concentration of the selected metal complex remained unaltered, for each addition of the DNA solution, the same volume of a double-concentrated metal complex solution was added.

Circular dichroism

CD spectra were recorded at 25 $^{\circ}\text{C}$ with the following parameters: range 600–220 nm, stop r: 0.2 nm, speed: 200 nm min⁻¹, accumulation: 4, response: 0.5 s, bandwidth: 1 nm. The titrations were carried out adding increasing amounts of a metal-complex stock solution to a DNA solution with constant concentration. To ensure that during the titration the concentration of the DNA remained unaltered, for each addition of the complex solution, the same volume of a double-concentrated DNA solution was added.

Computational details

The geometry of compounds **1** and **2** was fully optimized by DFT calculations, using the M06-2X DFT functional [26] and the dzvp basis set [27], as implemented in the Gaussian 09 program

package [28]. Selected structural parameters and Cartesian coordinates of both **1** and **2** are reported in the Supplementary material.

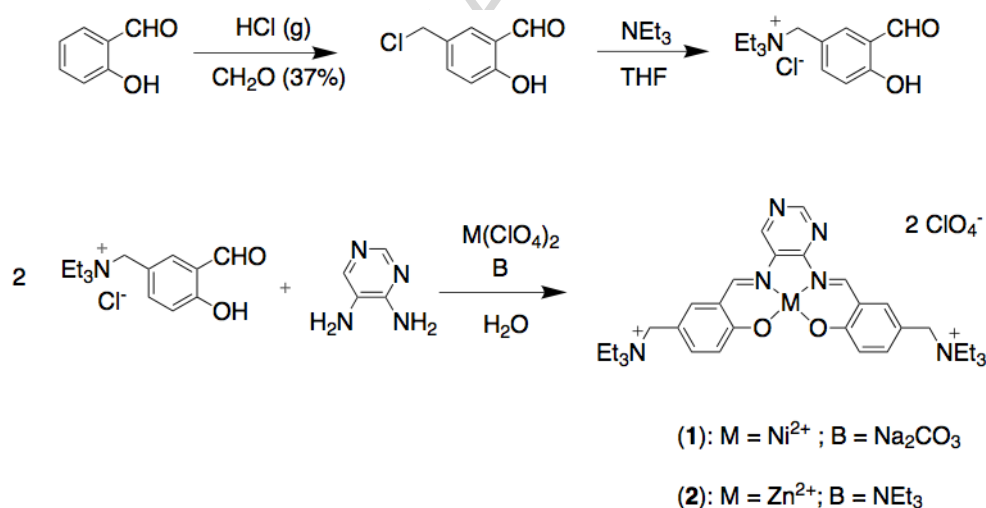
The interaction of complex **1** with the G4 model of the *hTelo* DNA (PDB ID 2HY9) [29] was investigated by molecular dynamics (MD) simulations, by following recently reported procedures [12,13,30]. Flanking bases, the first and the last two adenines, were deleted from the structure in order to use the experimental *hTelo*. MD simulations were performed with GROMACS 5.0.4 [31,32], using the Amber99 force field [33] with Parmbsc0 nucleic acid torsions [34]. The complex was positioned about 10 Å far over the 3' G-quartet, to simulate the molecular recognition process. The starting geometry and the partial atomic charges of **1** were calculated by using the M06-2X DFT functional [26] and the dzvp basis set [27]. To calculate atomic partial charges we have used the Restrained Electrostatic Potential (RESP) method [35]. Other intramolecular force-field parameters were generated with ACPYPE [36] and *parafreq* [37], respectively for the organic moiety and the metal center. A cubic box of TIP3P water molecules was added around the quadruplex to a depth of 1.0 nm on each side of the solutes. 19 K⁺ ions were added in order to neutralized the system, while other K⁺ and Cl⁻ ions were added to set the solution ionic strength to 0.15 M. Van der Waals parameters for nickel were taken from the UFF [38], while those for potassium cation were taken from the literature [39]. Explicit solvent simulations were performed in the isothermal-isobaric NPT ensemble, at a temperature of 300 K, under control of a velocity rescaling thermostat [40]. The particle mesh Ewald method was used to describe long-range electrostatic interactions [41]. A timestep of 2 fs was used for integration and all covalent bonds were constrained with the LINCS algorithm. There were two temperature coupling groups in these simulations: the first for the quadruplex and the metal complex, the second for water and ions. Preliminary MD simulations showed that the structure of the isolated metal complex is maintained in solution. Preliminary energy minimizations were run for 5000 steps with the steepest descend algorithm. During the equilibration, the metal

complex/quadruplex system was harmonically restrained with a force constant of $1000 \text{ kJ mol}^{-1} \text{ nm}^{-2}$, gradually relaxed into five consecutive steps of 100 ps each, to 500, 200, 100 and $50 \text{ kJ mol}^{-1} \text{ nm}^{-2}$. The Cartesian coordinates of the complex **1**/*hTelo* at the equilibrium are reported in the Supplementary file *1_hTelo.pdb*.

3. RESULTS AND DISCUSSION

Synthesis and characterization

Complexes **1** and **2** were synthesized as reported in Scheme 1 and characterized by NMR, IR and elemental analysis.



Scheme 1. Synthetic pathway for **1** and **2** perchlorate salts obtained with different bases (B).

DNA binding

To investigate the DNA binding of complexes **1** and **2** and, in particular, their selectivity towards G4, their UV-vis spectra were recorded in the presence of increasing amounts of 5'-(AGGGTT)₃AGGG-3' (*hTelo* G4) and double helical DNA (Figure 1).

The UV-vis spectra of both complexes present an intense absorption band at about 238 nm (black solid lines in Figure 1) and characteristic absorption bands in **1** (259 and 368 nm) and **2**

(275 and 385 nm). It is worth mentioning that, in Figure 1, the intensity increase occurring below 300 nm is attributable to DNA absorption.

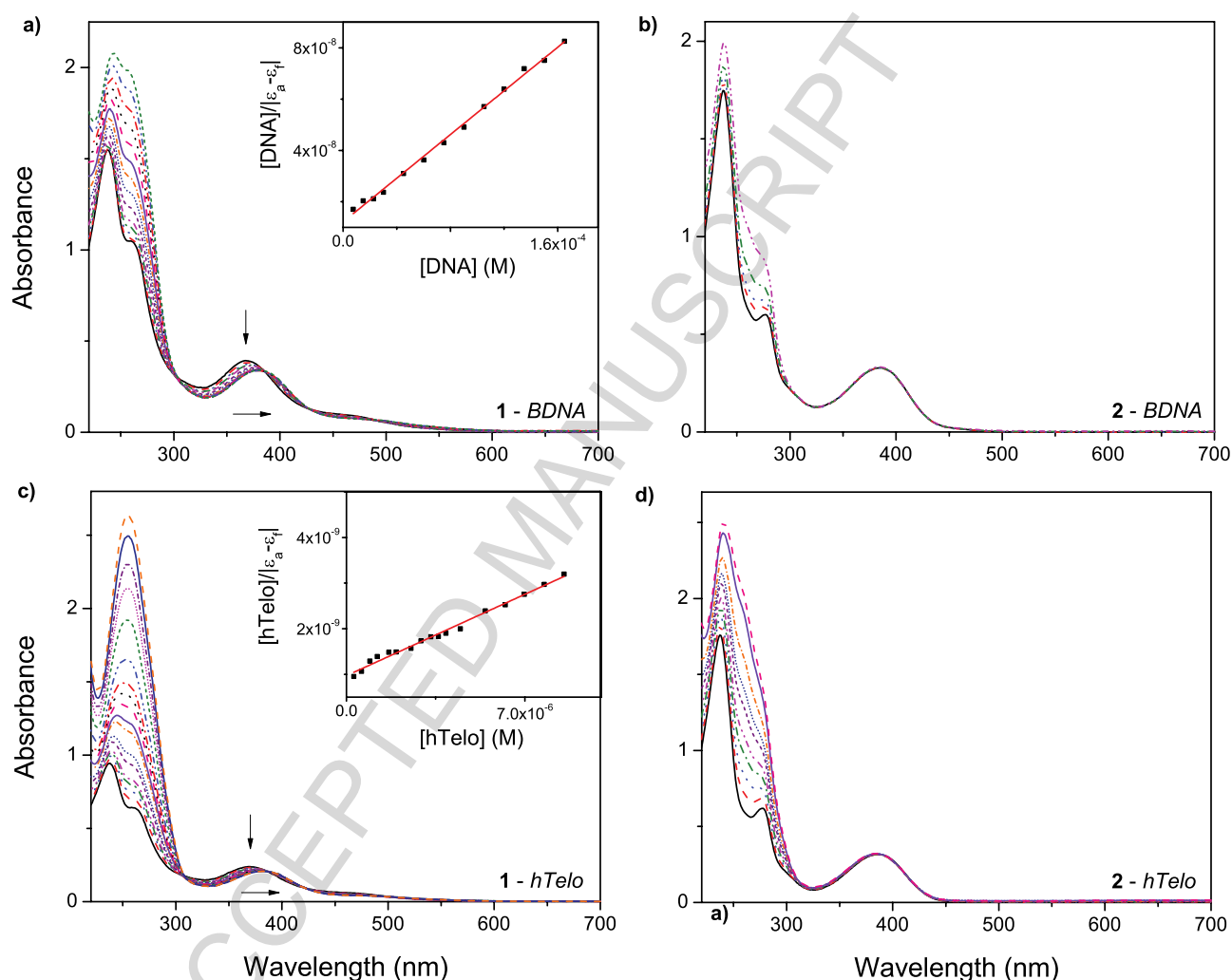


Figure 1. UV-vis spectra of **1** and **2**, collected in 100 mM KCl and 50 mM Tris-HCl buffer, in presence of increasing amounts of a,b) double helical DNA and c,d) *hTelo* G4. a) [**1**] = 31.0 μM , [$\text{DNA}_{\text{phosphate}}$] = 0.0 – 165.2 μM ; b) [**2**] = 29.5 μM ; [$\text{DNA}_{\text{phosphate}}$] = 0.0 – 92.7 μM ; c) [**1**] = 18.4 μM , [*hTelo* G4] = 0.0 – 8.5 μM ; d) [**2**] = 28.5 μM , [*hTelo* G4] = 0.0 – 6.4 μM . In the insets linear fits are shown, used to obtain binding constants between **1** and the polynucleotides.

The band at 385 nm of **2** is unperturbed by the presence of both duplex and G4 DNA in solution (Figure 1b,d), suggesting the absence of DNA-binding of the zinc(II) complex. On the other hand, the corresponding band at 368 nm of the nickel(II) complex **1** (Figure 1a,c) is

significantly modified upon addition of increasing amounts of both duplex-DNA (Figure 1a) and G4 (Figure 1c). In detail, the band is red shifted by about 15 nm and its intensity is reduced of about 20%, indicating that the electronic levels of the complex **1** are significantly perturbed upon the interaction with both duplex and G4 DNA.

These results reveal that the nature of the two metal ions and the slightly different structure of the two metal complexes, perfectly planar and tetrahedrally distorted, for nickel(II) and zinc(II) complexes, respectively, deeply affect the metal complex - DNA binding, as recently observed for similar Salen-like complexes [12,13]. In particular, in such complexes the presence of a zinc(II) ion always induced lower DNA-binding affinity than the presence of nickel(II).

It is known that the ionic strength increase induces a decrease in the binding strength between cationic metal complexes and the negatively charged DNA polymer. In particular, we have recently noticed that the decrease in the K_b values of zinc(II) complexes, induced by ionic strength, is larger than that observed for nickel(II) complexes [12,13]. Together with the results obtained in the present work, we can conclude that the dispersion (hydrophobic) contribution plays a bigger role than the Coulomb (hydrophilic) contribution in the non covalent binding between **1** and both duplex and G4 DNA.

To determine the intrinsic binding constant of the **1**/DNA systems, the quantity $[DNA]/|\epsilon_a - \epsilon_f|$ and $[hTelo]/|\epsilon_a - \epsilon_f|$ at 368 nm for **1** was plotted as a function of the molar concentration of respectively duplex DNA (inset in Figure 1a) and *hTelo* G4 (inset in Fig. 1c). The binding constants were obtained by plotting the data $[DNA]/|\epsilon_a - \epsilon_f|$ versus $[DNA]$ and finding the best linear fit using the following equation [13,15]:

$$\frac{[DNA]}{|\epsilon_a - \epsilon_f|} = \frac{[DNA]}{|\epsilon_b - \epsilon_f|} + \frac{1}{|\epsilon_b - \epsilon_f| \times K_b}$$

where the concentration of DNA is expressed as monomer units. In details, $\epsilon_a = A_{\text{observed}}/[ML^{2+}]$, ϵ_b is the extinction coefficient of the DNA bound complex, and ϵ_f is the extinction coefficient of

the free complex determined by a calibration curve of the isolated metal complexes in aqueous solution, following the Beer–Lambert law. The K_b values obtained by the linear fittings of the experimental data are $(3.5 \pm 0.3) \times 10^4 \text{ M}^{-1}$ and $(2.6 \pm 0.2) \times 10^5 \text{ M}^{-1}$. The DNA-binding constants were determined also by analysing the absorption data with the “intrinsic method” by Rodger and Nordén [42] (see Figures S9 and S10). The results summarized in Table 1 show that both methods provide similar K_b values and confirm that **1** binds tighter *hTelo* rather than duplex DNA, showing selectivity of one order of magnitude towards telomeric G-quadruplex with respect to double helical DNA.

Table 1. DNA-binding constant (K_b) values of **1** with duplex-DNA and *hTelo*-G4.

	Equation 1	Intrinsic method
Duplex-DNA	$(3.5 \pm 0.3) \times 10^4 \text{ M}^{-1}$	$(5.4 \pm 0.5) \times 10^4 \text{ M}^{-1}$
<i>hTelo</i>-G4	$(2.6 \pm 0.2) \times 10^5 \text{ M}^{-1}$	$(2.9 \pm 0.5) \times 10^5 \text{ M}^{-1}$

Being circular dichroism (CD) a technique highly sensitive to minor variations of the chiral structure of DNA [43-45], it can be used to monitor subtle changes after its interaction with small molecules [42,46]. For this reason, CD spectra of duplex DNA 50 μM solutions have been recorded in presence of increasing amounts of **1** (Figure 2a) and **2** (data not shown) up to a molar ratio [Complex]/[DNA] of about 0.8 and 0.9 respectively.

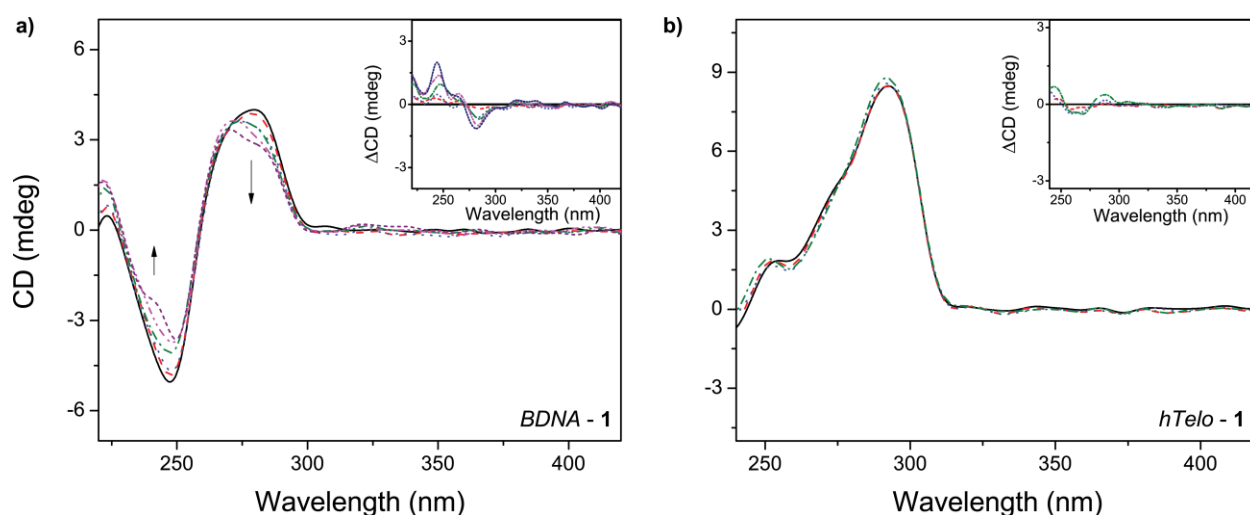


Figure 2. CD spectra of duplex-DNA (a) and *hTelo* G4 (b) collected in 100 mM KCl and 50 mM Tris-HCl buffer, in presence of increasing amounts of **1**. a) $[DNA_{\text{phosphate}}] = 50.0 \mu\text{M}$, $[1] = 0.0 - 38.9 \mu\text{M}$; b) $[hTelo] = 2.0 \mu\text{M}$, $[1] = 0.0 - 16.0 \mu\text{M}$. Difference CD spectra are shown in the inset.

The CD spectrum of duplex-DNA (Figure 2a) is slightly modified by the addition of **1** with intensity decrease of the characteristic positive and negative bands at 275 nm and 245 nm. This result remarks a loss of the typical chirality of duplex-DNA after its interaction with **1**, in agreement with helix unwinding after intercalation. Moreover, the CD spectrum of duplex-DNA is not affected by the addition of increasing amounts of **2** indicating the absence of structural modifications and confirming the absence of DNA-binding of the zinc(II) complex.

It is known that, in K^+ solutions, telomeric quadruplex adopts a hybrid structure with mixed parallel/antiparallel strands and it has been previously shown that some G4 binders may induce conformational modifications on quadruplex topology [47-49]. While the measurements of the UV-visible absorption revealed the occurrence of a tight binding in the **1**/*hTelo* complex, no significant change in CD spectra of *hTelo* G4 was noticed in presence of increasing amounts of complex **1** (Figure 2b), showing that such compound does not induce biomolecular conformational changes.

Lastly, the relative viscosities of a 350 μM concentrated solution of DNA in presence of increasing amounts of **1** and **2** up to the molar ratio (R_2) = 0.1, have been recorded (Figure 3).

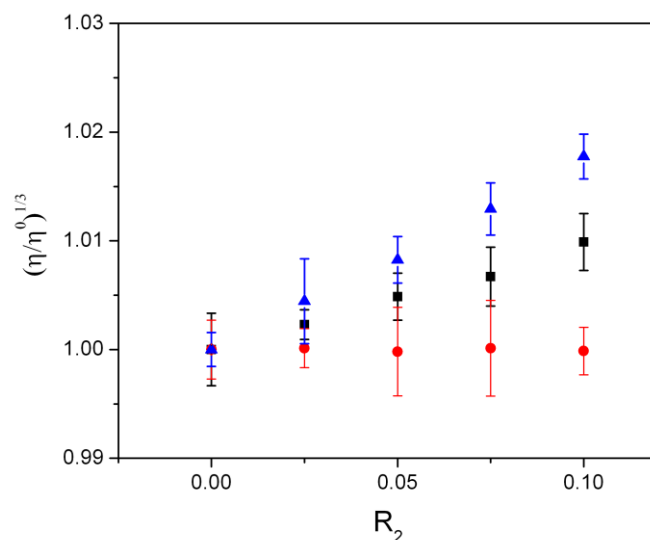


Figure 3. Relative viscosity of a 350 μM solution of duplex-DNA in presence of increasing amounts of **1** (black squares), **2** (red circles) and ethidium bromide (blue triangles).

The viscosity trend induced in the same experimental conditions by the DNA-intercalator ethidium bromide was added in Figure 3 for comparison. Figure 3 shows that the nickel(II) complex **1** causes a linear increase of the viscosity of duplex-DNA, a clear evidence of DNA-intercalation. As a matter of fact, an intercalative interaction increases the separation of the base pairs at the intercalation site causing an increase of DNAs' viscosity [12,50]. On the contrary, no modification of the relative viscosity of DNA is observed in presence of **2**, allowing to conclude that the zinc(II) complex, in the experimental conditions used to carry out these studies, does not interact with double stranded DNA.

Molecular Dynamics Simulations

A 250 ns MD simulation was performed in order to mimic the top-stacking interaction between **1** and a hybrid G4 model of the telomeric quadruplex. This model (pdb id 2HY9) was chosen

because it represents the most relevant G4 conformation adopted under the experimental conditions selected in the present work. The complex was placed about 10 Å far from the 3' G-quartet, to simulate the molecular recognition process. As expected, due to the electrostatic attraction between the negatively charged phosphate groups and the positively charged triethylammonium arms of the ligand, **1** suddenly reaches the 3' quartet.

The RMSD of the non-hydrogen atoms is shown in Figure 4. Such plot shows that G-quartets (green) are rigidly bound and undergo displacements of only ca. 0.5 Å around their equilibrium position during all simulation time. On the other hand, the large values of the all atoms RMSD (red) are essentially due to the large and continuous oscillations of the highly flexible loops and flanking bases.

In contrast to other G4 conformations, the 3' G-quartet is not easily accessible in this *hTelo* structure, since it is covered by a loop containing residues T11, T12 and A13. Figure 5 shows that, when **1** is close to the surface of the quadruplex, i.e. at 15 ns of the MD simulation, there is a stacking overlap between its planar portion (constituted by the three aromatic rings and by the nickel(II) ion) and the 3' quartet, with the pyrimidine group pointing toward the mentioned TTA loop.

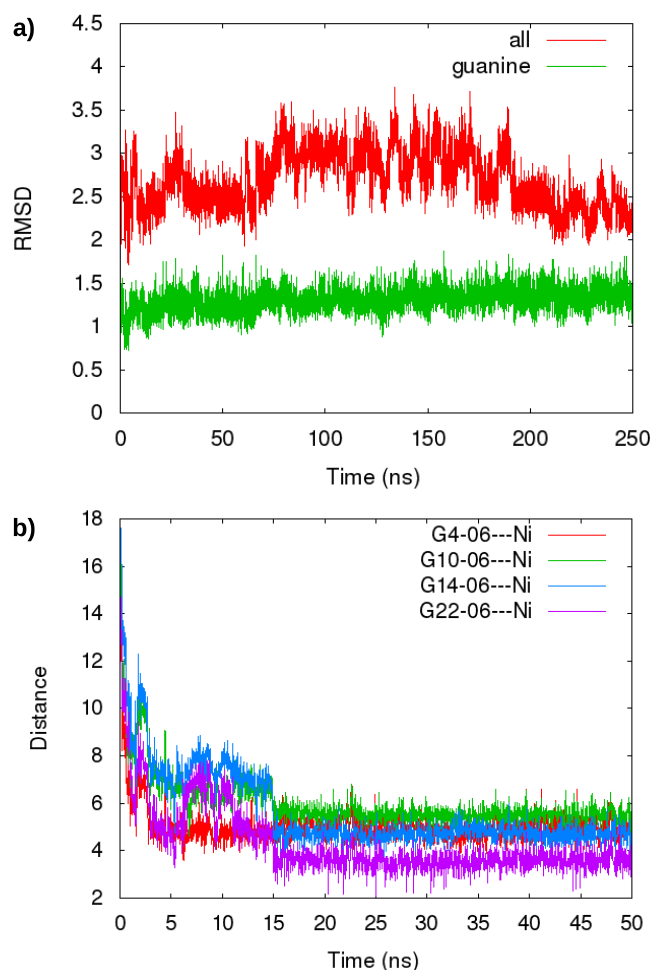


Figure 4: a) RMSD (\AA) of the non-hydrogen atoms, all residues (red line) and only guanines (green line); b) distance (\AA) between Ni and O6 atoms of the four guanines in the 3' quartet.

The distance between O6 atoms of the 3' quartet guanine bases and Ni is plotted in Figure 4b. In agreement with previous literature findings [13,15], during the simulation the metal complex roughly aligns the nickel atom with the potassium channel (see Figure 5b). However, as shown by Figure 5 and by the distance plot in Figure 4b, the metal is not equidistant from the four bases, because of the presence and steric hindrance of the TTA loop. The average distance with the closest oxygen is about 3.5 \AA , a value close to that observed in a previous work after QM/MM optimization of the whole structure of a similar nickel(II) complex with a *hTelo* G4 [13]. Such Ni-O interatomic distance indicates the absence of metal coordination and the occurrence of only van der Waals interactions in the stabilization of the **1**/*hTelo* complex.

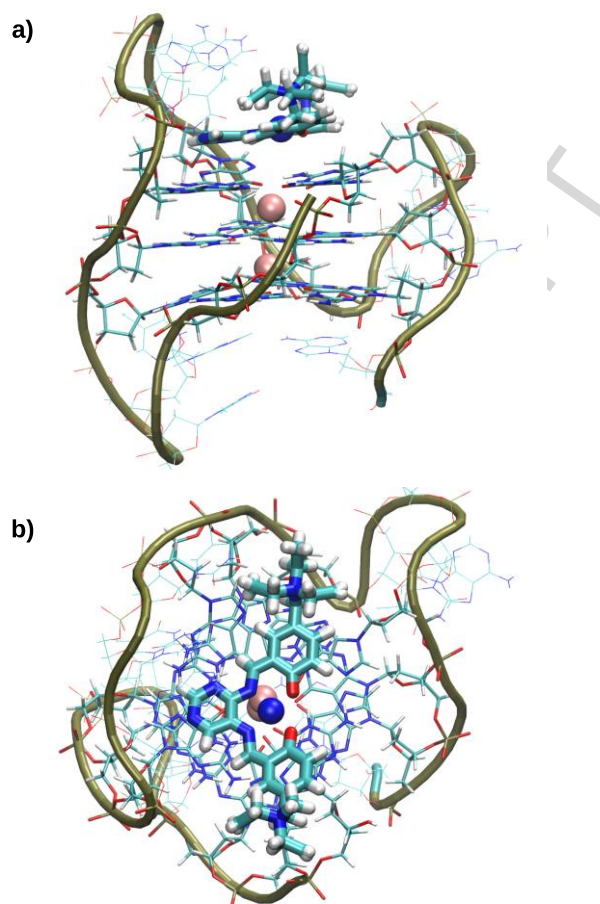


Figure 5: A representative snapshot showing a) side view and b) top view of the **1**-*hTelo* system.

4. CONCLUDING REMARKS

We have synthesized and characterized nickel(II) (**1**) and zinc(II) (**2**) complexes of a Salen-like ligand, carrying a pyrimidine ring on the N,N' bridge. The spectroscopic and hydrodynamic studies with duplex and G-quadruplex DNA led to the conclusion that only the Ni^{II} derivative interacts with both DNA secondary structures. The value of the experimental DNA-binding constant, K_b , for *hTelo* G4 is one order of magnitude higher than that for double helical DNA, confirming the G-quadruplex selectivity of such complex **1**.

The non-binding properties of the zinc(II) complex **2**, clearly points out that the choice of the coordinated metal ion is essential to determine the binding affinity with both duplex and G-

quadruplex DNA. In general, the results obtained confirm once more that nickel(II) Schiff base complexes show tighter DNA-binding affinity compared to analogous zinc(II) complexes.

Acknowledgements

European COST Action CM1105 is gratefully acknowledged. AT has received funding from the Mahlke-Obermann Stiftung and the European Union's Seventh Framework Programme for research, technological development and demonstration under grant agreement no 609431.

5. REREFENCES

- [1] M. Pradeep Kumar, S. Tejaswi, A. Rambabu, V.K.A. Kalalbandi, Shivaraj, *Polyhedron*. 102 (2015) 111–120.
- [2] A.C. Komor, J.K. Barton, *Chem. Commun.* 49 (2013) 3617–3630.
- [3] G. Barone, A. Terenzi, A. Lauria, A.M. Almerico, J.M. Leal, N. Busto, B. García, *Coord. Chem. Rev.* 257 (2013) 2848–2862.
- [4] P.G. Cozzi, *Chem. Soc. Rev.* 33 (2004) 410–421.
- [5] A. Silvestri, G. Barone, G. Ruisi, M.T. Lo Giudice, S. Tumminello, *J. Inorg. Biochem.* 98 (2004) 589–594.
- [6] A. Silvestri, G. Barone, G. Ruisi, D. Anselmo, S. Riela, V.T. Liveri, *J. Inorg. Biochem.* 101 (2007) 841–848.
- [7] G. Barone, N. Gambino, A. Ruggirello, A. Silvestri, A. Terenzi, V. Turco Liveri, *J. Inorg. Biochem.* 103 (2009) 731–737.
- [8] A. Terenzi, C. Ducani, L. Male, G. Barone, M.J. Hannon, *Dalton Trans.* 42 (2013) 11220–11226.
- [9] A. Terenzi, A. Lauria, A.M. Almerico, G. Barone, *Dalton Trans.* 44 (2015) 3527–3535.
- [10] A. Biancardi, A. Burgalassi, A. Terenzi, A. Spinello, G. Barone, T. Biver, B. Mennucci, *Chem. – Eur. J.* 20 (2014) 7439–7447.

- [11] G. Barone, A. Ruggirello, A. Silvestri, A. Terenzi, V.T. Liveri, J. Inorg. Biochem. 104 (2010) 765–773.
- [12] A. Lauria, R. Bonsignore, A. Terenzi, A. Spinello, F. Giannici, A. Longo, A.M. Almerico, G. Barone, Dalton Trans. 43 (2014) 6108–6119.
- [13] A. Terenzi, R. Bonsignore, A. Spinello, C. Gentile, A. Martorana, C. Ducani, B. Högberg, A.M. Almerico, A. Lauria, G. Barone, RSC Adv. 4 (2014) 33245–33256.
- [14] D.L. Ang, B.W.J. Harper, L. Cubo, O. Mendoza, R. Vilar, J. Aldrich-Wright, Chem. – Eur. J. (2015).
- [15] N.H. Campbell, N.H.A. Karim, G.N. Parkinson, M. Gunaratnam, V. Petrucci, A.K. Todd, R. Vilar, S. Neidle, J. Med. Chem. 55 (2011) 209–222.
- [16] S.M.H. Ali, Y.-K. Yan, P.P.F. Lee, K.Z.X. Khong, M.A. Sk, K.H. Lim, B. Klejevska, R. Vilar, Dalton Trans. 43 (2013) 1449–1459.
- [17] N.H.A. Karim, O. Mendoza, A. Shivalingam, A.J. Thompson, S. Ghosh, M.K. Kuimova, R. Vilar, RSC Adv. 4 (2013) 3355–3363.
- [18] G. Biffi, D. Tannahill, J. McCafferty, S. Balasubramanian, Nat. Chem. 5 (2013) 182–186.
- [19] T.-M. Ou, Y.-J. Lu, C. Zhang, Z.-S. Huang, X.-D. Wang, J.-H. Tan, Y. Chen, D.-L. Ma, K.-Y. Wong, J.C.-O. Tang, A.S.-C. Chan, L.-Q. Gu, J. Med. Chem. 50 (2007) 1465–1474.
- [20] S. Balasubramanian, L.H. Hurley, S. Neidle, Nat. Rev. Drug Discov. 10 (2011) 261–275.
- [21] J.L. Huppert, S. Balasubramanian, Nucleic Acids Res. 33 (2005) 2908–2916.
- [22] T.A. Brooks, S. Kendrick, L. Hurley, FEBS J. 277 (2010) 3459–3469.
- [23] A. Lauria, A. Terenzi, R. Bartolotta, R. Bonsignore, U. Perricone, M. Tutone, A. Martorana, G. Barone, A.M. Almerico, Curr. Med. Chem. 21 (2014) 2665–2690.
- [24] P. McPhie, Methods Enzymol. 22 (1971) 23–32.
- [25] M.E. Reichmann, S.A. Rice, C.A. Thomas, P. Doty, J. Am. Chem. Soc. 76 (1954) 3047–3053.

- [26] Y. Zhao, D.G. Truhlar, *Theor. Chem. Acc.* 120 (2008) 215–241.
- [27] N. Godbout, D.R. Salahub, J. Andzelm, E. Wimmer, *Can. J. Chem.* 70 (1992) 560–571.
- [28] M. Frisch, G. Trucks, H. Schlegel, G. Scuseria, M. Robb, J. Cheeseman, et al., *Gaussian 09*, Revis. A1 Gaussian Inc Wallingford CT. (2009).
- [29] J. Dai, C. PUNCHIHEWA, A. Ambrus, D. Chen, R.A. Jones, D. Yang, *Nucleic Acids Res.* 35 (2007) 2440–2450.
- [30] A. Spinello, G. Barone, J. Grunenberg, *Phys. Chem. Chem. Phys.* 18 (2016) 2871–2877.
- [31] D. Van Der Spoel, E. Lindahl, B. Hess, G. Groenhof, A.E. Mark, H.J.C. Berendsen, *J. Comput. Chem.* 26 (2005) 1701–1718.
- [32] B. Hess, C. Kutzner, D. van der Spoel, E. Lindahl, *J. Chem. Theory Comput.* 4 (2008) 435–447.
- [33] A. Pérez, I. Marchán, D. Svozil, J. Sponer, T.E. Cheatham III, C.A. Laughton, M. Orozco, *Biophys. J.* 92 (2007) 3817–3829.
- [34] A.T. Guy, T.J. Piggot, S. Khalid, *Biophys. J.* 103 (2012) 1028–1036.
- [35] C.I. Bayly, P. Cieplak, W. Cornell, P.A. Kollman, *J. Phys. Chem* 97 (1993) 10269–10280
- [36] A.W.S. da Silva, W.F. Vranken, *BMC Res. Notes.* 5 (2012) 1–8.
- [37] S.K. Burger, M. Lacasse, T. Verstraelen, J. Drewry, P. Gunning, P.W. Ayers, *J. Chem. Theory Comput.* 8 (2012) 554–562.
- [38] A.K. Rappe, C.J. Casewit, K.S. Colwell, W.A. Goddard, W.M. Skiff, *J. Am. Chem. Soc.* 114 (1992) 10024–10035.
- [39] I.S. Joung, T.E. Cheatham, *J. Phys. Chem. B.* 112 (2008) 9020–9041.
- [40] G. Bussi, D. Donadio, M. Parrinello, *J. Chem. Phys.* 126 (2007) 014101–7.
- [41] T. Darden, D. York, L. Pedersen, *J. Chem. Phys.* 98 (1993) 10089–10092.
- [42] A. Rodger, B. Nordén, *Circular dichroism and linear dichroism*, Oxford University

Press, Oxford; New York, 1997.

[43] M.J. Waring, *J. Mol. Biol.* 13 (1965) 269–274.

[44] A.I. Karsisiotis, N.M. Hessari, E. Novellino, G.P. Spada, A. Randazzo, M. Webba da Silva, *Angew. Chem. Int. Ed.* 50 (2011) 10645–10648.

[45] S. Paramasivan, I. Rujan, P.H. Bolton, *Methods.* 43 (2007) 324–331.

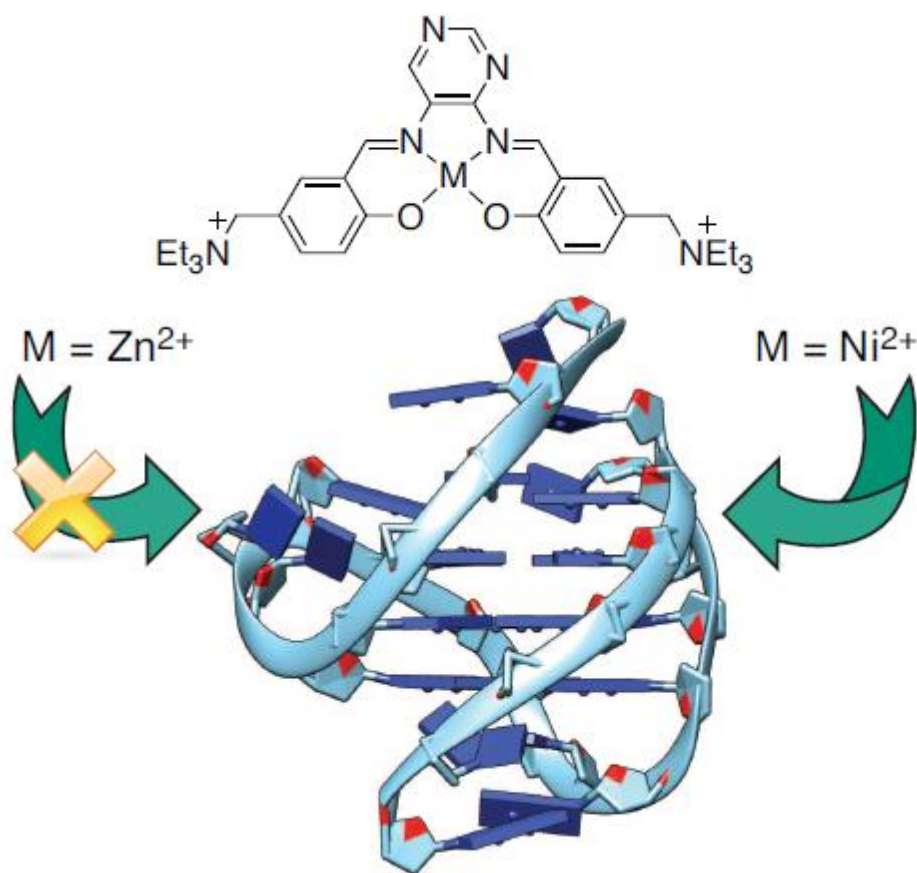
[46] J. Kypr, I. Kejnovská, D. Renčiuk, M. Vorlíčková, *Nucleic Acids Res.* 37 (2009) 1713–1725.

[47] K. Suntharalingam, A.J.P. White, R. Vilar, *Inorg. Chem.* 48 (2009) 9427–9435.

[48] J. Zhou, G. Yuan, *Chem. – Eur. J.* 13 (2007) 5018–5023.

[49] D.P.N. Goncalves, S. Ladame, S. Balasubramanian, J.K.M. Sanders, *Org. Biomol. Chem.* 4 (2006) 3337–3342.

[50] H.-L. Huang, Y.-J. Liu, C.-H. Zeng, L.-X. He, F.-H. Wu, *DNA Cell Biol.* 29 (2010) 261–270.



Graphical abstract

The right choice of the metal ion deeply influences the DNA-binding ability of Schiff base complexes: while the zinc(II) complex does not bind to DNA, the nickel(II) complex intercalates duplex-DNA and selectively binds G-quadruplex, by top-stacking.

Highlights

- Ni^{II} (**1**) and Zn^{II} (**2**) Schiff base complexes were synthesized and characterized.
- **1** binds to both G-quadruplex and duplex-DNA, by top-stacking and intercalation.
- **2** does not possess DNA-binding properties.
- **1** has G-quadruplex binding 10 fold stronger than duplex-DNA binding.
- The binding of **1** with G-quadruplex was mimicked by MD simulations.

ACCEPTED MANUSCRIPT